Effects of elevated $CO_2$ on MeHg and IHg in rice

Rachel J. Strickman [a,*], Sarah Larson [a,b], Yasmine A. Farhat [a,c], Van Anh T. Hoang [d], Sarah E. Rothenberg [d], Rebecca B. Neumann [a]

a Department of Civil and Environmental Engineering, University of Washington, Seattle, WA, 98195, USA

b USDA Forest Service, RMRS, Moscow Forestry Sciences Laboratory, Moscow, ID, 83843, USA

c Faculty of Agricultural and Food Sciences, American University of Beirut, Riad El Solh, Beirut, 1107 2020, Lebanon

d College of Health, Oregon State University, Corvallis, OR, USA

* Corresponding author.

E-mail address: strickma@uw.edu (R.J. Strickman).

Keywords:

Mercury

Methylmercury

Elevated carbon dioxide

Rice

Contamination

ABSTRACT

Methylmercury (MeHg) and, to a lesser extent, inorganic mercury (IHg) contamination of rice is a global public health concern, but little is known about how soil and grain Hg concentrations respond to elevated CO2 (ECO2) or how ECO2 alters movement of Hg through the soil-plant-grain system. To advance knowledge of how Hg contamination of rice will change in the future, this study explored the effect of elevated CO2 (ECO2, c. 800 ppm) on soil, iron plaque, root, stem/leaf, and grain concentrations of MeHg and IHg. We observed evidence that ECO2 increased accumulation of MeHg, but not IHg, in rice grain. For IHg, ECO2 did not alter its uptake from the soil, translocation through the plant, or concentration in rice grain. However, ECO2 did reduce uptake of IHg from the air into leaf tissues, likely as a result of the reduced stomatal conductivity and thus more limited direct uptake from the air.

Methylmercury concentrations in the grain of plants grown at ECO2 were significantly higher than those of plants grown at ambient CO2. Moreover, MeHg concentrations were also elevated in stem/leaf (82 %) and root tissue (37 %) for ECO2 plants, although the root-tissue results were not statistically significant. In contrast, soil MeHg concentrations were virtually indistinguishable between treatments, indicating that higher rice grain MeHg concentrations were not likely due to higher microbial IHg methylation in soil. Plant uptake of MeHg into stem/leaves and grain from the soil was significantly greater in the ECO2 treatment; however, translocation patterns of MeHg within the plant itself did not differ between treatments. Notably, these patterns existed despite consistently lower transpiration in the ECO2 treatment, and thus less mass flow of solute towards and through the plant. Our results indicate that as CO2 concentrations rise, the human health risks related to MeHg in grain will likely increase.

## 1. Introduction

Mercury (Hg) is a highly toxic pollutant that contaminates nearly every environment. The total Hg load of the water, soil, and biota is dominated by inorganic Hg (IHg). A small fraction of Hg is present as an organometal, methylmercury (MeHg; Beckers and Rinklebe, 2017), which is produced in aquatic environments by IHg methylating microbiota (Bravo and Cosio, 2019). The toxicity of Hg varies depending on its speciation (Beckers and Rinklebe, 2017). Methylmercury is neurotoxic; low-level MeHg exposure, which mainly occurs via aquatic-sourced food including fish and rice, causes subtle but irreversible intellectual deficits for children exposed in utero (Karagas et al., 2012; Rothenberg et al., 2021). While IHg exposure through food has received less attention than MeHg (Viˇsnjevec et al., 2014), there are concerns about its kidney toxicity and other negative effects (Beckers and Rinklebe, 2017; Bernhoft, 2012; Clarkson and Magos, 2006; Syversen and Kaur, 2012).

Rice agroecosystems are an important component of human exposure to Hg. MeHg accumulates in rice (Hylander and Goodsite, 2006; Rothenberg et al., 2014) to levels that adversely impact child neurodevelopment in some populations consuming a heavily rice-based diet (Rothenberg et al., 2021). Emphasizing the urgency of this issue, rice represents c. 10 % of the intake of MeHg worldwide (Liu et al., 2019), and is currently the staple food of more than three billion people, a number which is expected to rise to five billion by 2030 (Khush, 2005). Rice also represents a dietary source of IHg; unlike seafood, 21–88 % of total Hg in rice is present as IHg (Rothenberg et al., 2014; Wang et al., 2020; Xu et al., 2019). Two studies have found that residents of a Hg-contaminated area in China may experience impairment of kidney function as a result of IHg exposure directly from rice (Li et al., 2015a; Zhang et al., 2020).

Rising atmospheric CO2 levels, which may reach 550–800 ppm by 2100 (IPCC, 2021), have the potential to alter both the MeHg and IHg content of soil and their movement through the soil-plant-grain system. Firstly, elevated CO2 may alter microbial methylation in the soil, which is the source of MeHg to rice grain (Aslam et al., 2022; Strickman and Mitchell, 2017), through increased rice root exudation (Baek, 2011) which in turn stimulates microbial methylation in rice paddies (Windham-Myers et al., 2009; Zhao et al., 2018). ECO2 can also increase the mobilization of IHg (Pierce et al., 2022), potentially stimulating methylation through increased IHg supply. Secondly, elevated CO2 could affect the movement of both MeHg and IHg from soil and air towards plant tissues. Dissolved MeHg is transported to the plant root surface via the movement of porewater (mass flow) which is driven by the transpirational uptake of water by the plant. Mass flow and solute uptake tend to decrease in high-CO2 conditions because plants narrow their stomatal aperture as the photosynthetic demand for carbon can be met with a smaller volume of air (Ainsworth and Rogers, 2007; Keenan et al., 2013; Kumar et al., 2017), potentially altering MeHg availability for uptake. IHg is partially taken up from soil solution via mass flow, but is also absorbed as gaseous mercury directly through the stomata (Aslam et al., 2022; Meng et al., 2012; M. Meng et al., 2014; Tang et al., 2021; Zhou et al., 2015). ECO2 could therefore alter plant IHg uptake through both changes in mass flow and stomatal aperture.

Elevated CO2 could also change the total amount as well as the absorptive capacity of iron plaque, a layer of iron oxyhydroxide compounds that coats rice roots (Zandi et al., 2023). Plaque intercepts and binds IHg and MeHg (Tiffreau et al., 1995), serving as a protective barrier against uptake (Li et al., 2017; Li et al., 2015; Wang et al., 2015). Elevated CO2 can alter the characteristics of the iron plaque by decreasing the Eh and pH in soil porewaters through changes in plant physiology and associated microbial responses (Wang et al., 2023; Yang et al., 2022). These changes occur as a result of higher exudation of carbon from plant roots, which increases microbial activity and results in more reduced conditions (Cheng et al., 2010), and increased plant release of carbonic acids (Wu et al., 2009) and protons to maintain charge balance after the uptake of basic nutrients (Zhang et al., 2018). These changes could lead to more iron in the plaque (Yang et al., 2023), because more acidic porewater pH facilitates the release of additional Fe (II), which is oxidized to solid forms of Fe(III) in the oxic rhizosphere (Yang et al., 2022). This enhancement of iron content of plaque could reduce uptake of MeHg and IHg to above-ground tissues. In addition, ECO2-related shifts in eH and pH can alter the crystallinity of the iron plaque towards more amorphous iron species (Yang et al., 2022), but it is not known how this process affects MeHg and IHg uptake to the plant.

Finally, ECO2 might alter the concentrations of Hg in plant tissue compartments between the plaque and the grain. The mechanism by which MeHg enters the plant and is translocated is not know, but it appears to be bound to cysteine residues (Hao et al., 2022; Meng et al., 2014; Xu et al., 2016). Some MeHg is photo-demethylated within aboveground plant tissues (Xu et al., 2016), some remains bound in the leaves at maturity (Meng et al., 2011; 2010), and some is transported into developing grain as a pseudo-nutrient. ECO2 generally lowers the protein content of rice grain while raising the carbohydrate content, which could perturb the pseudonutrient-based translocation of MeHg (Wang et al., 2011). IHg which is not bound to root tissues or iron plaque is translocated upwards through the plant. However, gaseous Hg is also taken up directly from the atmosphere by leaves in the course of gas exchange, and subsequently oxidized to IHg (Aslam et al., 2022; Meng et al., 2012; 2010; Strickman and Mitchell, 2017). Gaseous uptake could be inhibited by the reduced stomatal conductivity that accompanies ECO2. IHg from both of these sources is translocated to grain, but IHg in the air can also directly enter grain via intercalation with thiol-bearing protein moieties (Aslam et al., 2022; Meng et al., 2014).

Despite the many routes by which ECO2 could alter Hg in rice grain, only two studies have examined this question. The only study to explore the effect of ECO2 on MeHg in rice grain found a statistically nonsignificant doubling of grain MeHg concentrations at 550–600 ppm CO2 (Mao et al., 2021). The effect of ECO2 on IHg is inconsistent, with one study observing a decrease in grain IHg content under 550 ppm (Tang et al., 2021), while Mao et al. 2021 found no effect. Neither study explored the effect of ECO2 on the soil or iron plaque compartments, and both used ECO2 settings (500–600 ppm) associated with SSP2–4.5, which projects an “intermediate” scenario for climate change (Aslam et al. 2021). The influence of CO2 concentrations greater than 600 ppm on MeHg behavior in the soil-plant-grain system has not been investigated, despite the urgency of understanding the effects of more dramatically elevated $CO_2$ levels associated with the “high” climate change scenario, SSP3–7.0 (Huard et al., 2022).

To address this knowledge gap, we grew rice plants under ambient (c. 400 ppm, as of 2018; $ACO_2$) and highly elevated (c. 800 ppm; $ECO_2$) $CO_2$ concentrations, then compared MeHg and IHg in the soil, plaque, roots, stem/leaves, and grain to identify the direction and magnitude of perturbations in the concentrations and movement of MeHg through the soil-plant-grain system.

## 2. Materials and methods

### 2.1. Soil collection, plant propagation, and rhizobox planting

Rice plants were cultivated in growth chambers during December–May of 2017–2018 at the University of Washington Center for Urban Horticulture (47◦39'27" N, 122◦17'21" W; 10 m above sea level). Soil was collected in September 2017 from a rice paddy field at the University of California Davis, California, USA. Soil storage and homogenization, and rhizobox construction and preparation, are described in Strickman et al., 2022. The background concentrations of MeHg was 0.01–0.12 ng/g, and of IHg, 0.068–0.25 ng/g (Strickman et al., 2022). This experiment used M-206, a short-season Calrose-type Japonica rice variety (Farhat et al., 2021). Seedlings were pre-cultivated in agar for 22 days, as in Strickman et al. 2022. Dates are noted as the day after planting (DAP).

On DAP 23, seedlings were transplanted into paddy soil in shallow rhizoboxes (25 × 5 × 50 cm inner dimensions) fitted with removable facings. Six rhizoboxes were maintained in each of two chambers, with one chamber at ambient $CO_2$ ($ACO_2$ treatment; c. 400 ppm in 2017–2018) and the other supplemented to 800 ppm $CO_2$ (elevated $CO_2$, $ECO_2$ treatment). Planting details are available in Supplementary Text 1. 2.2. Plant growing conditions and physiological monitoring

Work was conducted in custom growth chambers (210 × 110 × 110 cm) fitted with ventilation, lighting, temperature and humidity control, and the capacity to adjust $CO_2$ concentrations. Complete details of chamber construction are available in (Rho et al., 2020). Chambers were housed adjacent to one another inside a climate-controlled greenhouse and drew air from the same outdoor source.

Supplemental $CO_2$ was supplied via a compressed gas tank connected with Tygon tubing, and assessed every 2-3 days using a PP Systems WMA-4 $CO_2$ Analyzer (PP Systems International, Amesbury, Massachusetts). Further information is available in Supplementary Text 2. Plants were illuminated by natural light supplemented with compact fluorescent lights on a 16H day, 8H night cycle. Photosynthetically active radiation ranged between c. 200 to 700 μmol/m2/s. Temperatures were within the range of 28–32∘C in the day and 23–27∘C night for both chambers. The overlying layer of Hoaglands solution was supplemented as necessary, with a layer of 5 cm maintained at all times.

Humidity was controlled, but not equalized between chambers. Until tillering, humidity adjustments were used to equalize transpiration between treatments; thereafter, relative humidity was held constant at the last settings (80 % for ECO2 treatment, 45 % for ACO2). Transpiration data were collected 2-3 times weekly and averaged across plant growth stages: seedling (DAP 23–41), early tillering (DAP 42–58), peak tillering (59–89), booting (DAP 90–96), flowering (DAP 97–107), and grain filling (DAP 108–135/142). See supplementary Text 3 for full details.

Photosynthetic rate measurements were collected at tillering (DAP 89) and grain maturity (DAP 135) stages using a LI-COR 6400XT portable photosynthesis system (LI-COR Biosciences, Nebraska, USA) with the following settings: leaf temperature 30∘ C, humidity of c. 30 %, and PAR 200 μmol/m2/s. The LI-COR CO2 setting were 440 ppm for ACO2, and 830 ppm for ECO2.

## 2.3. Sample collection

Plant tissue and soil samples were collected when plants had reached maturity. Grains in the ECO2 treatment were collected on DAP 135, while ACO2 was harvested on DAP 142. Working on the bench, grains were removed, and then the rhizoboxes opened to collect soil samples with acid-washed plastic scrapers, and immediately flash-frozen on dry ice; these samples were stored at -80 ∘C and lyophilized. Soil samples were not oven dried and therefore include both the solid phase and the soil water. Following soil collection, plants were gently separated into root and stem/leaf biomass. Stem/leaves and roots were washed with copious tap water and rinsed with DI water. All plant tissues were frozen at -4 ∘C and preserved by lyophilization.

## 2.4. Sample analyses

### 2.4.1. Plant tissue preparation

Hulled, unpolished rice grains were pooled by box and ground to a fine powder using a ceramic mortar; stem/leaf tissues were homogenized in a steel coffee grinder while roots were snipped with steel scissors. Separate sets of equipment were used for each treatment. All equipment was cleaned between samples with a Kim wipe dampened with ethanol and jet of nitrogen. Roots were separated into two portions of approximately equal weight. One portion was analyzed with the iron plaque intact, while the other was stripped of its iron plaque coating using a citrate-bicarbonate-dithionite extraction technique (Taylor and Crowder, 1983, Supplementary Text 4). This process enabled separate determination of MeHg and THg content in root biomass and iron plaque.

2.4.2. Mercury and iron determinations

Methylmercury and total mercury (THg) were measured in soil, plaque, root, stem/leaf, and grain compartments. Due to COVID-19 disruptions, two analytical facilities were used. The THg and MeHg concentrations of grains and soil were determined at Oregon State University in 2018. Total Hg and MeHg concentrations of plaque, stem/ leaves, and roots were determined at the University of Toronto in 2021.

Soil THg analyses were conducted using EPA Method 7473 (United States Environmental Protection Agency, 2007) based on AAS via a Lumex RA 915+ Pyro 915 Mercury Analyzer; samples were directly combusted without acid digestion. Grain THg samples were quantified using the EPA Method 1631 (United States Environmental Protection Agency, 2002) based on cold vapor atomic fluorescence spectrometry (CVAFS) (MERX-T with Brooks Rand Model III instrument, Brooks Rand Instruments, Seattle, WA, USA) and a hot nitric-sulfuric acid digestion (see Supplementary Text 5 and Rothenberg et al., 2015).

Soil and grain MeHg analyses were performed using solvent extraction and EPA 1630 (United States Environmental Protection Agency, 2001) with gas chromatography (GC)-CVAFS using a (Model-III Detector, Brooks Rand Instruments, Seattle, WA). Soil for MeHg analysis was digested using KBr, H2SO4, and CuSO4 solution, with MeHg subsequently partitioned to dichloromethane, and finally back-extracted to an aqueous solution for analysis (Bloom et al., 1997) See Supplementary Text 5 for more details.

Methylmercury concentrations of the washed and unwashed roots, as well as of the stem/leaf tissues, were determined using isotope dilution-gas chromatography-inductively coupled plasma mass spectrometry (Hintelmann et al., 2000). THg concentrations in the same sample compartments were determined using isotope dilution-cold-vapor-ICP-MS. Sample preparation and analytical techniques are described in Strickman et al. (2022).

Instruments for Hg determinations at Oregon State University were calibrated daily with a coefficient of variation (r2) >0.99. At both facilities, the quality of THg and MeHg determinations was assessed using percent recovery of standard reference materials and matrix spikes, relative percent difference between duplicates (RPDs), and method detection limits; these data are available in Table 1.

Inorganic Hg (IHg) concentrations were estimated by subtracting MeHg from THg concentrations. MeHg and THg contents of the iron plaque were expressed as the difference between the concentration in the intact root and the iron-stripped root. This concentration represents the MeHg or THg bound in the plaque compartment of the intact root, on a dry weight basis, and assuming that iron plaque weight was negligible. Plaque iron concentration was estimated as the difference between iron content of stripped and unstripped roots. This method was chosen because of shipping restrictions on the citrate-bicarbonate-dithionite solution. Iron measurements were made using an Agilent ICP-MS at the University of Toronto.

### 2.5. Bioaccumulation factors and transfer factors

Bioaccumulation and transfer factors were calculated to explore how MeHg and IHg moved through the soil-plant-grain system. Transfer factors measure movement within the plant between the iron plaque, roots, stem/leaves, and grain (Buscaroli, 2017), and are calculated as the ratio of sink concentration (Csink) to the concentration of the relevant source compartment (Csource):

$$TFi = Csink / Csource$$

Bioaccumulation factors are the quotient of MeHg or IHg concentration in the plant tissue (Ci) to the concentration in the soil (Csoil), and assess accumulation in plant tissues, with soil as the primary source (Buscaroli, 2017)

$$BAFi = Ci / Csoil$$

### 2.6. Statistical analyses

Variables were assessed for normality using a combination of q-q plots, frequency distribution histograms, and comparison of median and mean values. Variables were transformed as necessary to approximate a normal distribution. Individual variables were compared between treatments using a two tailed student's T test. Statistical analysis was conducted with R version 3.3.1 (R Core Team, 2016). Normalized and non-normalized data is available at Mendeley Data at DOI:10.17632/sgj3bbdvv2.1.

## 3. Results and discussion

### 3.1. Effect of CO2 on plant growth and physiology

Carbon dioxide treatments strongly affected the physiology of the plants. Photosynthetic rates were 40 % higher in the ECO2 treatment than in the ACO2 treatment at tillering ($p = 0.01$) and c. 70 % higher at grain maturity ($p = 0.22$) (Table 2). This degree of photosynthetic stimulation is comparable with previous work using identical growth chambers and with similar CO2 conditions at the panicle initiation stage (Rho et al., 2020).

**Table 1**

QA/QC for mercury and methylmercury determinations.

| | Method | Standard reference material | SRM Recovery (mean ± st. dev, N) | RSD (mean ± st. dev., N) | Spike Recovery (mean ± st. dev, N) | MDL (ng/g) |
|---|---|---|---|---|---|---|
| MeHg (grain) | EPA 1630 | TORT2 (lobster) | 99 ± 14 (2) | 20 ± 4.0 (3) | 96 ± 26 (2) | 0.002 |
| MeHg (leaves and roots) | IC-GC-ICPMS | IAEE-158 | 102 ± 3.6 (6) | 2.90 ± 2.44 (4) | | 0.004 |
| MeHg (soil) | EPA 1630 | TORT2 (lobster) | 91 ± 0.33 (2) | 25 ± 17 (4) [1] | | 0.002 |
| THg (grain) | EPA 1631 | NIST 1568b (rice) | 114 ± 18 (2) | 7.4 ± 0.94 (2) | 91 ± 3.7 (2) | 0.001 |
| | | IAEA-086 (hair) | 86 ± 4.4 (2) | | | |
| THg (leaves and roots) THg | IC-GC-ICPMS | MESS-4 | 83 ± 3.65 (4) | 4.36 ± 6.58 (4) 16 | 104 ± 8.59 (4) | 0.0009 |
| (soil) | EPA 7473 | NIST 1515 (apple leaves) | 88 ± 3.6 (4) | 25 ± (9)[2] | | 3 |
| | | TORT2 (lobster) | 95 ± 3.6 (4) | | | |

Detection limits for MeHg and THg in stem/leaves and roots were assessed as three times the standard deviation of blank concentrations, which were calculated using average sample masses. Detection limits for all other samples were assessed as the lowest point on the calibration curve corrected for the average mass of the sample. All values exceeded the associated MDL. The average relative standard deviation between duplicates (RSD) was calculated as the ratio of the standard deviation to the average recoveries of each duplicate pair expressed as a percentage).

[1] When one sample was removed, the RSD was 21 ± 15 (n = 3) [2] When 2 samples were removed, the RSD was 19 ± 12 (n = 7)

**Table 2**

Photosynthetic rate assessed on DAP 89 and 135/142, and stomatal conductance, transpiration rate, and humidity settings averaged over seedling, early tillering, peak tillering, booting, flowering, and grain maturity growth stages. Data is presented separately for the $ECO_2$ (Elevated) and $ACO_2$ (Ambient) treatments. Stomatal conductance for seedling stage was not recorded. Full data is available in Table S1.

| Days after planting (DAP) | | Photosynthetic rate, A μmol $CO_2$/m$^2$/sec | Stomatal conductance, $G_s$ mmol $H_2O$/m$^2$/s | Transpiration rate, E mmol $H_2O$/m$^2$/s | Humidity setting (average) % RH |
|---|---|---|---|---|---|
| Tillering harvest | Elevated | 14.27 ± 0.959 | | | |
| DAP 89 | Ambient | 10.2 ± 3.13 | | | |
| Grain maturity harvest | Elevated | 9.3 ± 2.68 | | | |
| DAP 135/142 | Ambient | 5.5 ± 2.07 | | | |
| Seedling | Elevated | | | 1.36 ± 0.74 | 50% |
| DAP 23–41 | Ambient | | | 0.84 ± 0.47 | 50% |
| Early tillering | Elevated | | 243.1 ± 53 | 1.89 ± 0.48 | 50% |
| DAP 42–58 | Ambient | | 258.9 ± 46.8 | 2.12 ± 0.52 | 50% |
| Peak Tillering | Elevated | | 223.4 ± 41.8 | 2.42 ± 0.62 | 50–80% |
| DAP 59–89 | Ambient | | 331.8 ± 45.9 | 4.12 ± 0.77 | 45–60% |
| Booting | Elevated | | 176.7 ± 39.3 | 1.64 ± 0.56 | 80% |
| DAP 90–96 | Ambient | | 299.9 ± 63.1 | 3.61 ± 1.04 | 45% |
| Flowering | Elevated | | 209.5 ± 38.4 | 2.12 ± 0.5 | 80% |
| DAP 97–107 | Ambient | | 353 ± 66.3 | 4.38 ± 1.1 | 45% |

| | | | | | | | | |
|---|---|---|---|---|---|---|---|---|
| Grain maturity | Elevated | 149.8 | ± | 17.9 | 1.38 | ± | 0.23 | 80% |
| DAP 108–135/142 | Ambient | 286.3 | ± | 28.4 | 3.35 | ± | 0.44 | 45% |

As anticipated, transpiration responded rapidly to differences in both humidity and CO2 concentrations. One of the original experimental goals was to assess uptake and movement of MeHg under ECO2 conditions in the absence of transpirational differences between treatments. Early in the plants' life histories, transpiration was successfully equalized between treatments by progressively raising the humidity in the ECO2 treatment while lowering the relative humidity in the ACO2 treatment (Table S1). Low-humidity conditions prompted the plants in the ACO2 treatment to narrow the stomatal aperture in order to reduce water loss, mimicking the lower stomatal conductivity of plants in the ECO2 treatment. This approach was successful at seedling and early tillering growth stages, where averaged transpiration rates were not significantly different between treatments ($p = 0.27$ and 0.44 respectively). However, the humidity-based equalization technique became ineffective past DAP 68 of the experiment, at approximately the point the plants entered the full tillering phase. This outcome is likely because air leakage from the chamber made it impossible to raise chamber humidity beyond 80 % and rapid growth drove high transpiration rates (Hidayati et al., 2016). After this point, transpiration was consistently and significantly lower in the ECO2 treatment (Table S1). The differential in transpiration between ECO2 and ACO2 varied over the plant's life cycle from peak tillering (-41 %), booting (-55 %), flowering (-52 %), and grain maturity (-59 %; $p = 0.001$–0.002, Table 2).

Stomatal conductivity followed a very similar pattern to transpiration over the course of the experiment. Stomatal conductivity was consistent between treatments at early tillering ($p = 0.60$), but thereafter diverged and became significantly lower in the ECO2 compared to the ACO2 treatments (-33 % – -48 %, $p = 0.001$– 0.003) (Table 2). These differences in both transpiration and stomatal conductivity in ECO2 vs ACO2 are comparable to previous work that grew rice in ambient and elevated (500–800 ppm) conditions (Ikawa et al., 2018; Rho et al., 2020; Shimono et al., 2013; Tang et al., 2021). We conclude that, despite humidity manipulations, the stomatal conductivity of the plants (and associated rates of transpiration) were still broadly representative of rice plant physiology under elevated CO2.

### 3.2. Effect of ECO2 on MeHg in the soil-plant-grain system

#### 3.2.1. Soil MeHg

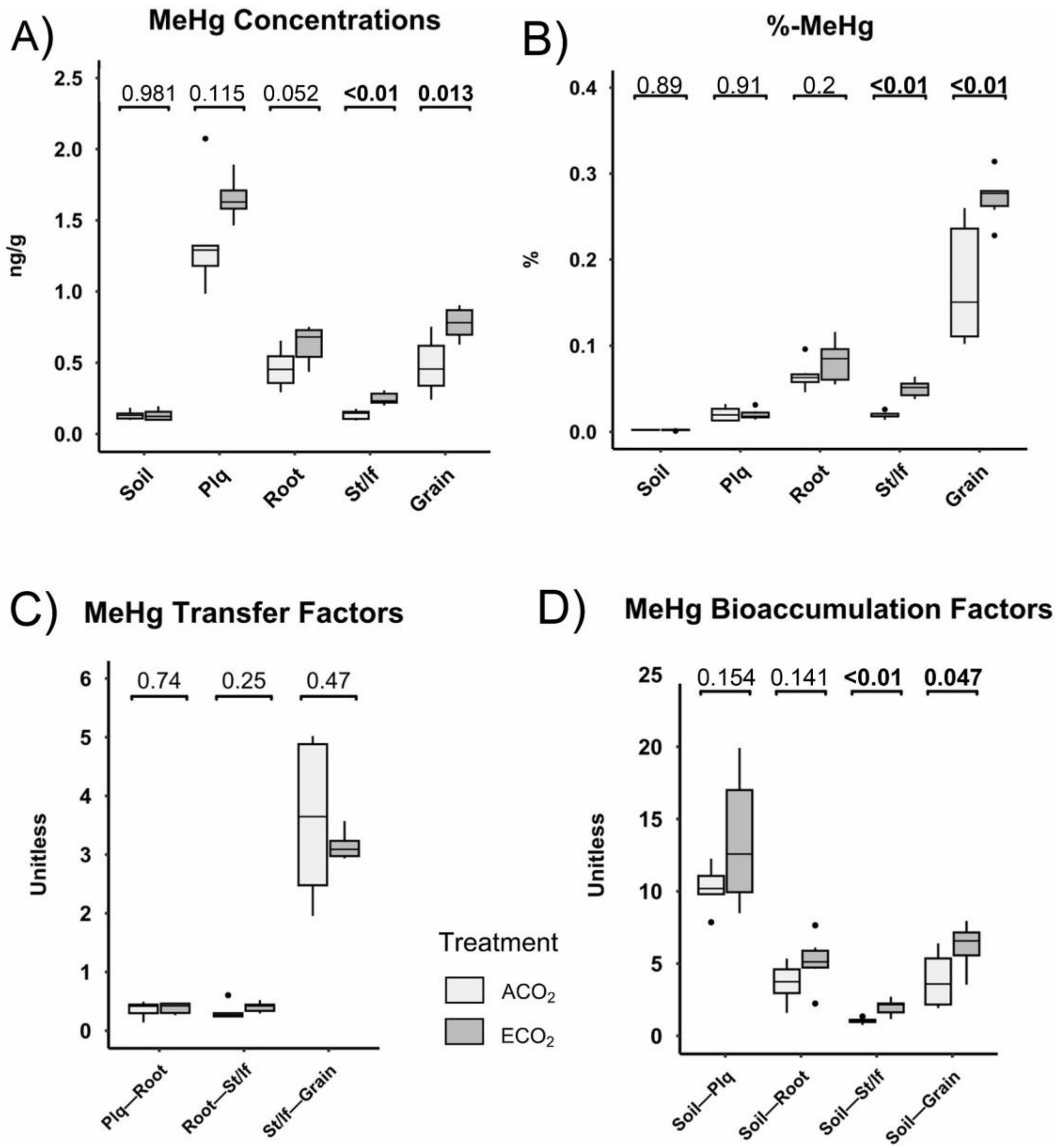


*Fig. 1. MeHg concentrations, %-MeHg values, and MeHg bioaccumulation and transfer factors in the soil-plant-grain system. All graphs compare the ECO2 and ACO2 treatments. A) MeHg concentrations in soil, iron plaque, root tissue without plaque, stem/leaf (st/lf), and grain, (B) %-MeHg values, (C) MeHg transfer factors within the plant with source compartment listed first and sink compartment listed second along the x-axis, (D) MeHg bioaccumulation factors within the plant with the source (soil) listed first and the sink listed second along the x-axis. For this, and all subsequent figures: Data presented is untransformed. P-values of T-tests (based on normalized data) are displayed above each pair of boxplots. The shaded area of each figure represents the 75th to 25th interquartile range (IQR); the central line represents the median; whiskers represent the highest data value that falls below 1.5x the IQR. Dots represent data falling beyond 1.5x the IQR.*

Contrary to expectations, there was no evidence that ECO2 affected MeHg concentrations in soil, which ranged between 0.10–0.20 ng/g ($p = 0.98$, Fig. 1A). This finding is important because this is the first study to explore the effect of ECO2 on MeHg production in soil, and because the responsiveness of methylation to climate change is a key uncertainty in managing Hg on a global scale (Chen et al., 2018). Methylation did occur during the experiment as evidenced by increases in soil MeHg concentrations from 0.09 ng/g prior to planting (Strickman et al., 2022) to a mean of 0.13 ± 0.03 ng/g at grain maturity. We therefore conclude that MeHg production, while occurring in this system, was not impacted by elevated CO2. Supporting this interpretation, the %-MeHg values, a rough estimate of the methylation capacity of a system, did not differ between treatments (Fig. 1B, $p = 0.89$). This finding suggests that atmospheric CO2 concentrations are less important to alterations in soil MeHg production than secondary aspects of climate change, such as altered temperature (Yang et al., 2016) or hydrology (Haynes et al., 2019).

3.2.2. Iron plaque Fe and MeHg

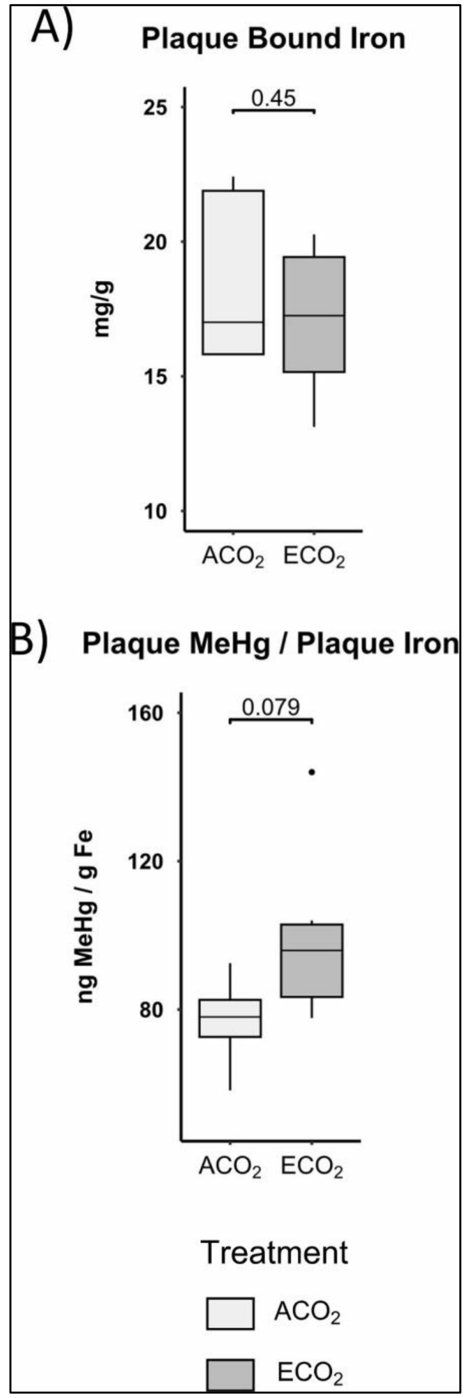


*Fig. 2. (A) Plaque-bound iron concentrations per root biomass, and (B) ratio of plaque-bound MeHg to plaque iron, compared between ECO2 and ACO2 treatments.*

The effect of ECO2 on MeHg accumulation in plaque was inconclusive. Previous work has observed that higher concentrations of Fe in root plaque are negatively related to the MeHg (Li et al., 2017; Li et al., 2015) and IHg (Wang et al., 2015; 2014; Zhou and Li, 2019) concentrations of aboveground tissues, including grain. This makes the effect of ECO2 on iron content in plaque an important issue. In our study, mean concentration of iron in plaque, normalized by root biomass, was similar between treatments (17.09 ± 2.85 mg/g ECO2, 18.59 ± 3.29 mg/g ACO2; $p = 0.45$, Fig. 2 A), suggesting that ECO2 did not alter the total formation of iron plaque on roots in our experiment. Despite the similar iron contents in plaque, it was notable that both MeHg concentration in plaque, and the MeHg/Fe ratio in plaque, were numerically different between treatments. Mean plaque MeHg was 22 % higher in ECO2 compared to ACO2, while the MeHg/Fe ratio of plaque was 30 % greater in ECO2 (Figs. 1A and 2B). While both of these results fell below the threshold of significance ($p = 0.115$–$0.079$), we note that a single outlier in the ACO2 treatment was responsible for this result. When the outlier was removed, both plaque MeHg concentration and MeHg/Fe ratio were significantly higher in the ECO2 treatment ($p < 0.01 – 0.04$). This observation tentatively suggests that ECO2 may have altered the effectiveness of the iron plaque as a barrier to MeHg in comparison to previous studies, all of which were performed at ambient CO2 (Li et al., 2017; Li et al., 2015; Wang et al., 2015, 2014; Zhou and Li, 2019). The reason for the outlier could not be determined, but we note that the plaque MeHg concentration was higher than the treatment average (2.07 ng/g vs. 1.35 ng/g) while the root MeHg levels were lower than the treatment average (0.29 ng/g vs. 0.46 ng/g). The iron content of the plaque in the outlier was the highest observed in the study (22.42 mg/g). These patterns suggest an alteration in the formation of iron plaque and/or iron cycling in this individual replicate, which could be the result of many factors including unusually high root radial oxygen loss, which facilitates Fe plaque formation (Maisch et al., 2019); differences in the native soil Fe pool; or simply a more finely branched root architecture that had a higher surface area (Verma et al., 2022). Given the importance of iron plaque as an interceptor of MeHg uptake to rice plants (Li et al., 2017; Li et al., 2015), any potential reduction in the efficiency of this process is of interest. More investigation of the effect of ECO2 on MeHg binding to iron plaque is warranted, and should include careful study of the soil, porewater, microbiome, and plant physiological factors that could alter Fe cycling.

### 3.2.3. Root and stem/leaf MeHg

ECO2 increased the concentration of MeHg in stem/leaf tissue, and may have increased MeHg in roots. ECO2 did significantly increase the concentrations of MeHg in stem/leaf tissue ($0.25 \pm 0.04$ ng/g in ECO2 vs $0.14 \pm 0.03$ ng/g in ACO2; $p < 0.01$, Fig. 1A). Root MeHg concentrations ranged between 0.29 and 0.75 ng/g (Fig. 1A) and were 37 % higher in the ECO2 treatment than in the ACO2 treatment, a result that was at the threshold of significance ($p = 0.052$). In both treatments, stem/leaf MeHg was lower than root MeHg (Fig. 1A), likely reflecting the binding of MeHg in the root tissue itself, perhaps in apoplastic barriers, a process which is known to bind IHg (Wang et al., 2015). This observation is consistent with previous studies that explored MeHg distribution within the rice plant (Liu et al., 2021; M. Meng et al., 2014; Strickman and Mitchell, 2017; Zhou et al., 2015). The root–stem/leaf MeHg transfer factors were similar between treatments ($p = 0.25$, $0.40 \pm 0.09$ in ECO2 vs. $0.32 \pm 0.14$ in ACO2), indicating that the effectiveness of this binding process was insensitive to CO2 concentrations.

### 3.2.4. Grain MeHg

Methylmercury concentrations in grain in the ECO2 treatment were significantly higher (0.78 ± 0.11 ng/g) than ambient CO2 (0.48 ± 0.20 ng/g, $p = 0.013$). The magnitude and direction of this change is in concurrence with Mao et al. (2021), who observed an increase of rice grain MeHg from 2.5 ng/g at ambient CO2 (410–445 ppm) to 5 ng/g at 550–600 ppm ECO2. Although Mao et al.'s observation was not statistically significant, the current study provides greater statistical power (N=6 vs. N=3) and, in addition, used a higher CO2 concentration in the ECO2 treatment (800 vs. 550–600 ppm). Our findings indicate that highly elevated CO2 concentrations increase the MeHg burden of rice grain.

This result has concerning implications for human health in a changing climate. Methylmercury is already a threat to rice-consuming populations (Rothenberg et al., 2021, 2021; Wang et al., 2021; Wu et al., 2018). Rising CO2 may increase the MeHg concentration of these rice supplies and thus the dietary MeHg intake of consumers who are already experiencing negative health effects. In addition, ECO2- related increases in rice grain MeHg concentration may cause rice supplies that are currently near the provisional tolerable weekly intake (PTWI; Wang et al., 2021; 2020) to exceed that threshold. Notably, the PTWI may itself be an underestimate as it is based on fish intake, which supplies additional micronutrients that rice does not (Rothenberg et al., 2013); fish also has a lower intake efficiency of MeHg than does rice (Li et al., 2015b). Moreover, rice does not contain the same beneficial nutrients as fish, such as omega-3 fatty acids, which support brain development and may offset MeHg toxicity (European Food Safety Authority, 2012). Thus, MeHg toxicity has been observed at a lower MeHg exposure levels, compared to most studies among fish consumers (Rothenberg et al., 2021; 2016; 2014). Finally, the observation that more MeHg accumulates in grain in a high CO2 environment must be taken in combination with other effects of climate change, particularly temperature. In this study, temperature was equalized between both treatments in order to focus our questions on a single climate driver (CO2), since Hg methylation usually increases with temperature (Ullrich et al., 2001). Interactions between ECO2 and temperature have been found to create an additive increase in rice grain concentrations of arsenic (Muehe et al., 2019). These facts suggest that ECO2 combined with elevated temperature might have compounded effects on rice grain MeHg by increasing methylation in the soil.

### 3.2.5. Reasons for CO2 perturbation of MeHg accumulation in grain

A key finding of our work is that grain MeHg levels were greater in the ECO2 treatment, despite similar levels of bulk soil MeHg. The origin of the excess MeHg in grain at ECO2 must therefore lie with differences in mobilization and uptake from the soil-porewater system, transport through plant compartments, or both. The bioaccumulation factors (movement from soil to other compartments) and transfer factors (movement between plant tissue compartments) shed light on these questions. Firstly, we observed no evidence for any change in within-plant movement of MeHg. No significant differences were found between the transfer factors for plaque-root, root-stem/leaf, or stem/leaf- grain ($p = 0.25–0.74$, Fig. 1C). Therefore, the explanation for differential grain MeHg concentrations must be increased uptake from the soil system. This idea is supported by the observations that the soil-stem/leaf bioaccumulation factors were 91 % higher in the ECO2 treatment compared to the ACO2 treatment ($1.99 \pm 0.57$ vs. $1.04 \pm 0.20$, $p < 0.01$), while soil-grain bioaccumulation factors were 60 % higher in the ECO2 treatment compared to the ACO2 treatment (Fig. 1D, 6.21 ±

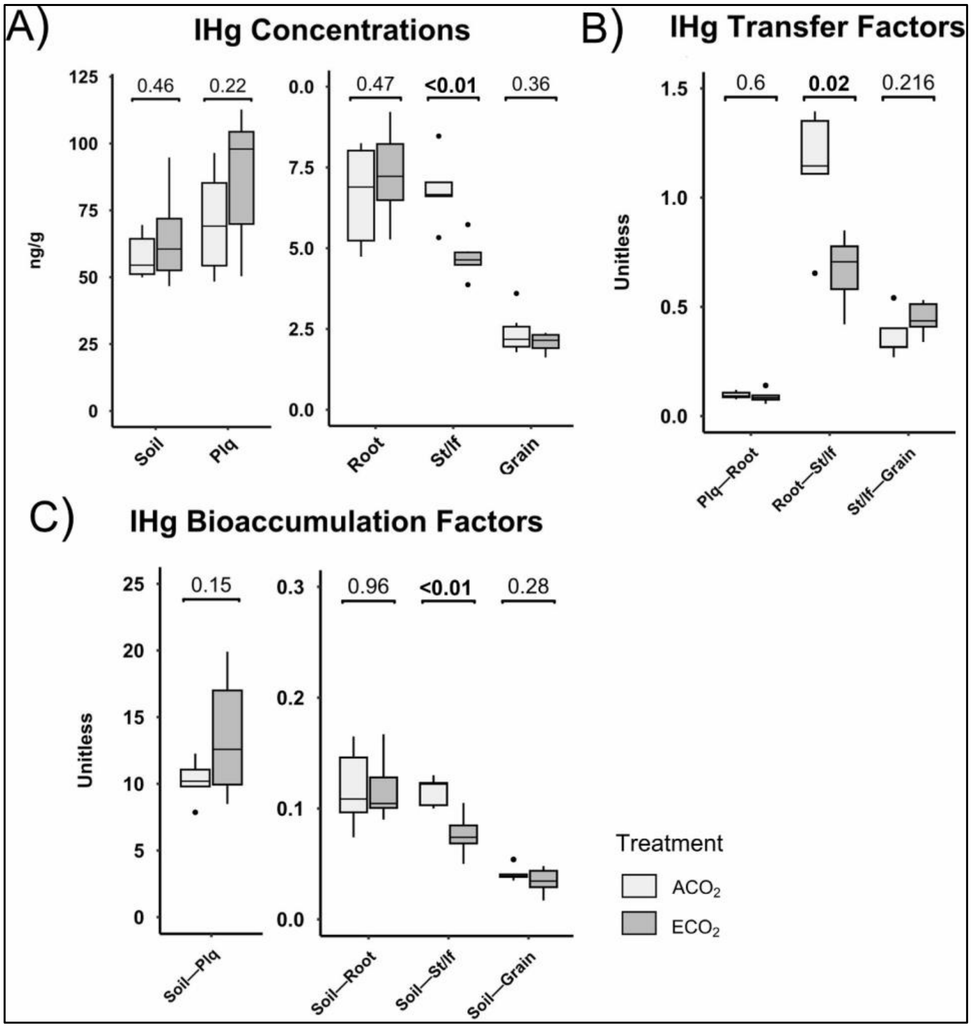


Fig. 3. IHg concentrations, bioaccumulation factors, and transfer factors in the soil-plant-grain system. All graphs compare the ECO2 and ACO2 treatments. (A) IHg concentrations; from left to right, paired boxplots comparing IHg concentrations in soil, iron plaque, roots, stem/leaf (st/lf), and grain. (B) IHg transfer factors between each compartment and the soil with the source compartment listed first and the sink compartment listed second along the x-axis. (C) IHg bioaccumulation factors within the plant with the source (soil) listed first and the sink listed second along the x-axis.

1.59 vs. 3.86 ± 1.96, $p = 0.047$). These findings indicate that at ECO2 more MeHg had moved from the soil system to stem/leaf and grain compartments. We conclude that changes in availability and absorption of MeHg from the soil, rather than changes in translocation within the plant itself, were the cause of increased MeHg in grain under elevated CO2.

Our work offers two insights on the mechanisms behind enhanced uptake of MeHg in ECO2 conditions. Firstly, our results demonstrate that any reduction in mass flow at ECO2 were insufficient to overcome the other drivers which increased MeHg availability and uptake. Despite humidity adjustments, transpiration rates in the ECO2 treatment were significantly lower than the ACO2 treatment after early tillering (Table S1), validating that mass flow would have been lower in the ECO2 treatment and would inhibit MeHg delivery to roots.

Rather, we suggest that the higher MeHg bioaccumulation in ECO2 may be related to changes in soil porewater MeHg concentrations. While our whole soil MeHg measurements did not differ between treatments, porewater and solid phase MeHg were not distinguished in this study. ECO2 has been observed to increase the porewater concentrations of other minerals in rice paddies because of changes in pH and Eh (Guo et al., 2012). Our soil MeHg measurements were based on whole soil samples that included solid phase as well as the solutes of porewater; in most soils, including rice paddies, sorption to thiol groups in the soil (Benoit et al., 1999) means that the solid phase concentrations of MeHg are many times greater than the aqueous phase concentrations (Rothenberg and Feng, 2012). This multiple-orders-of magnitude difference in porewater versus soil concentrations likely obscured any significant differences in porewater MeHg concentrations. It is therefore possible that the MeHg concentrations in solution were elevated enough to offset the reduced transpiration-driven mass flow and subsequent uptake to the plant, although further research is needed to explore this possibility.

### 3.3. Effect of ECO2 on inorganic mercury in the soil-plant-grain system

#### 3.3.1. Soil, plaque, and roots

Elevated carbon dioxide did not affect the soil, plaque, or root concentrations of IHg, or its movement through these compartments. Soil IHg concentrations (overall mean of 61 ng/g; Fig. 3) were representative of the Yolo Bypass in California, the region from which the soil originated (Tanner et al., 2018), and did not differ between treatments ($p = 0.46$), indicating that homogenization was effective in equalizing IHg supply. IHg concentrations in root iron plaque were greater than those in soil, with an overall mean of c. 80 ng/g, demonstrating that the plaque accumulated IHg from the soil, but that CO2 treatment had no effect on this process ($p = 0.22$). Root IHg concentrations (4.74–9.22 ng/g) were approximately 9 % of the plaque concentrations, and were also unaffected by CO2 treatment ($p = 0.47$). Furthermore, we observed no differences in the movement of IHg from plaque to root (bioaccumulation factors; $p = 0.6$, Fig. 3B), or from soil to plaque (transfer factors; $p = 0.15$, Fig. 3C) on the basis of treatment. We conclude that the effectiveness of the iron plaque as a barrier to IHg was not affected by ECO2 treatment. The importance of the iron plaque as a reservoir for IHg, however, suggests that alterations to iron plaque formation linked to other aspects of climate change, such as temperature (Farhat et al., 2021; Neumann et al., 2017) might alter its capacity to serve as a reservoir of IHg.

### 3.3.2. Stem/Leaf

ECO2 reduced the concentration of IHg in stem/leaf tissue, the only change observed in the entire soil-plant-grain system (4.71 ± 0.61 ng/g ECO2, 6.82 ± 1.13 ng/g ACO2). Stem/leaf IHg concentrations were c. 30 % lower in the ECO2 treatment ($p < 0.01$), in concurrence with previous work (Tang et al., 2021). This pattern is likely a result of the lower stomatal conductance in ECO2 conditions (Table 2), which allowed less atmospheric IHg to enter the mesophyll space (Aslam et al., 2022). This interpretation is strongly supported by the consistently lower stomatal conductance in the ECO2 treatment, which was significantly different past tillering ($p < 0.001$–$0.002$, Table 2). Although the soil-stem/leaf bioaccumulation factors were significantly lower in the ECO2 treatment ($p < 0.01$, Fig. 3C), suggesting a soil origin of IHg, we note that there was no change in the soil-root or soil-grain bioaccumulation factors ($p = 0.96, 0.28$). Given the mechanistic explanation of reduced stomatal conductivity, we believe that reduced uptake from air is the more likely explanation for the finding of lower IHg in stem/leaf tissue. Similar results have been observed in other grasses (Millhollen et al., 2006), and trees (Natali et al., 2008) as well as rice (Tang et al., 2021), suggesting that reduced stem/leaf IHg uptake in high CO2 conditions is widespread and may alter the global sequestration of IHg from the atmosphere into stem/leaf tissues. If climate change results in consistently reduced stomatal conductance across diverse plant communities, terrestrial deposition via litterfall will likely decrease in importance. This observation is also relevant to understanding the effect of climate change on the global Hg cycle, as approx. 2/3 of total terrestrial IHg is deposited through the decomposition of plant tissues, which absorb gaseous Hg0 directly from the atmosphere (Zhou and Obrist, 2021).

### 3.3.3. Grain

Grain IHg concentrations ranged between 1.62 and 3.60 ng/g, levels that are similar to previous field studies of rice in the Yolo Bypass (Tanner et al., 2018). Grain IHg was virtually indistinguishable between treatments (Fig. 3A, $p = 0.36$). This observation concurs with the work of Mao et al. (2021), but contrasts with that of Tang et al. (2021), who observed a 10 % decrease in grain IHg at 550 ppm ECO2 compared to ambient (400 ppm). This difference could be due to varietal differences in rice grain starch content, which hosts the S moieties that bind IHg (Meng et al., 2014). Although further work is needed on different rice cultivars, and in field conditions, it appears that elevated CO2 does not affect the accumulation of IHg in rice grain.

Our observation that grain IHg concentrations did not differ in ECO2 has implications for understanding human IHg exposure via rice. While grain IHg was consistent between treatments, there was a sharp treatment level differences in IHg of stem/leaves. The reduced atmospheric uptake of IHg in the leaves of ECO2 plants did not translate to lower IHg concentration in grain (Aslam et al., 2022; B. Meng et al., 2014). Previous work has disagreed on whether the IHg in rice grain is taken up directly from the atmosphere (Meng et al., 2014; Strickman and Mitchell, 2017) or if translocation from leaves and roots contributes to the grain IHg burden (Aslam et al., 2022). Our evidence suggests that a) IHg translocation from leaves to grain is a less important pathway than direct atmospheric uptake, and b) that elevated atmospheric CO2 does not affect the atmospheric uptake of IHg to grain. Therefore, in the absence of changes in local atmospheric IHg concentrations, the IHg burden of rice is unlikely to rise in response to elevating CO2.

## 4. Conclusion

We observed no effect of ECO2 on the IHg concentrations of most compartments, including soil, plaque, roots, and grain. Additionally, the movement of IHg from soil to most plant compartments, and within the plant itself, was unaffected by ECO2 treatment. We therefore infer that the grain burden of IHg is unlikely to change in response to rising CO2. A notable exception to this pattern, however, was the lower accumulation of IHg in rice stem/leaf tissue in response to decreased stomatal conductivity. The effect of ECO2 on atmospheric uptake of IHg to plant tissues, and subsequent deposition to terrestrial ecosystems, has implications for understanding the global mercury cycle and for the return of atmospheric Hg to the biosphere.

Grain MeHg was significantly higher in the ECO2 treatment. Our results suggest that gross MeHg supply in the soil was not altered, nor was the transfer of MeHg through the plant. These processes therefore cannot explain the differences in grain MeHg. Rather, extraction of MeHg from the soil seemed to be enhanced in the ECO2 treatment, based on significantly higher leaf-soil and grain-soil bioaccumulation factors, as well as possible increases in accumulation of MeHg on the protective root plaque layer. Given the importance of iron plaque in intercepting MeHg, the effect of ECO2 on plaque MeHg-sorption capacity should be explored in a greater range of soil types and degrees of MeHg contamination. MeHg sequestration in root tissue appeared to remain intact based on similar root-stem/leaf factors. Notably, increased uptake of MeHg occurred under ECO2 despite a reduction in transpiration, and thus mass flow of solutes towards the roots. We suggest that the increased uptake may be explained by differences in MeHg concentrations in porewater. More work is needed to understand the effect of both ECO2 and other climate drivers—notably temperature—on the behavior of IHg and MeHg in the soil, porewater, and plaque compartments of the plant-soil-grain system.

## CRediT authorship contribution statement

Rachel J. Strickman: Conceptualization, Methodology, Investigation, Formal analysis, Writing – original draft. Sarah Larson: Methodology, Investigation. Yasmine A. Farhat: Investigation, Writing – review & editing. Van Anh T. Hoang: Investigation. Sarah E. Rothenberg: Writing – review & editing, Resources. Rebecca B. Neumann:

Investigation, Writing – review & editing, Supervision.

## Declaration of competing interest

The authors declare that they have no known competing financial interests or personal relationships that could have appeared to influence the work reported in this paper.

## Data availability

Normalized and non-normalized data is available at Mendeley Data at https://doi.org/10.17632/sgj3bbdvv2.1.

## Acknowledgments

We would like to thank Dr. Nicholas Waldo for his assistance in the collected rice paddy soil used in this experiment; soil collection was facilitated by Professor Bruce Linquist of University of California Davis. We would like to thank Professor Soo-Hyung Kim and Dr. Hyungmin (Tony) Rho for access to and assistance with the CO2-controlled chambers and LI-COR measurement apparatus. We are grateful for the analytical excellence of Professor Carl Mitchell and Dr. Planck Huang during the preparation of root, stem/leaf, and iron samples. We would also like to thank Mikaela Balkind, Theresa Wong, and Annie Billotta who provided assistance and advice in the greenhouse and laboratory. This work was funded by National Science Foundation Grant EAR- 1740839 from the Government of the United States.

Supplementary materials

Supplementary material associated with this article can be found, in the online version, at doi:10.1016/j.envadv.2024.100515.

References

Ainsworth, E.A., Rogers, A., 2007. The response of photosynthesis and stomatal conductance to rising [CO2]: mechanisms and environmental interactions. Plant Cell Environ. 30, 258–270. https://doi.org/10.1111/j.1365-3040.2007.01641.x.

Arias, P.A., Bellouin, N., Jones, R.G., Naik, V., Plattner, G.K., Rogelj, J., Sillmann, J., Storelvmo, T., Thorne, P.W., Trewin, B., Rao, K.A., Adhikary, B., Allan, R.P.,

Armour, K., Barimalala, R., Canadell, J.G., Cassou, C., Cherchi, A., Collins, W.,

Corti, S., Cruz, F., Dentener, F.J., Dereczynski, C., Luca, A.D., Diongue, A., Doblas- Reyes, F.J., Dosio, A., Douville, H., Engelbrecht, F., Fyfe, J.C., Gillett, N.P., Goldfarb, L., 2021. Climate Change 2021: The Physical Science Basis. Contribution of Working Group I to the Sixth Assessment Report of the Intergovernmental Panel on Climate Change. n.d. Technical summary, in. Cambridge University Press, pp. 33–144.

Aslam, M.W., Meng, B., Abdelhafiz, M.A., Liu, J., Feng, X., 2022. Unravelling the interactive effect of soil and atmospheric mercury influencing mercury distribution and accumulation in the soil-rice system. Sci. Total Environ. 803, 149967 https://doi.org/10.1016/j.scitotenv.2021.149967.

Baek, W.J., 2011. Sequestration of roots-derived carbon in paddy soil under elevated CO2 with two temperature regimes as assessed by isotope technique. J. Korean Soc. Appl. Biol. Chem. 54, 403–408. https://doi.org/10.3839/jksabc.2011.063.

Beckers, F., Rinklebe, J., 2017. Cycling of mercury in the environment: sources, fate, and human health implications: a review. Crit. Rev. Environ. Sci. Technol. 47, 693–794. https://doi.org/10.1080/10643389.2017.1326277.

Benoit, J.M., Gilmour, C.C., Mason, R.P., Heyes, A., 1999. Sulfide controls on mercury speciation and bioavailability to methylating bacteria in sediment pore waters.

Environ. Sci. Technol. 33, 951–957. https://doi.org/10.1021/es9808200.

Bernhoft, R.A., 2012. Mercury toxicity and treatment: a review of the literature.

J. Environ. Public Health 2012, 460508. https://doi.org/10.1155/2012/460508.

Bloom, N.S., Colman, J.A., Barber, L., 1997. Artifact formation of methyl mercury during aqueous distillation and alternative techniques for the extraction of methyl mercury from environmental samples. Fresenius J. Anal. Chem. 358, 371–377. https://doi.

org/10.1007/s002160050432.

Bravo, A.G., Cosio, C., 2019. Biotic formation of methylmercury: A bio–physico–chemical conundrum. Limnol. Oceanogr. 11366 https://doi.org/ 10.1002/lno.11366 lno.

Buscaroli, A., 2017. An overview of indexes to evaluate terrestrial plants for phytoremediation purposes (Review). Ecol. Indic. 82, 367–380. https://doi.org/ 10.1016/j.ecolind.2017.07.003.

Chen, C.Y., Driscoll, C.T., Eagles-Smith, C.A., Eckley, C.S., Gay, D.A., Hsu-Kim, H.,

Keane, S.E., Kirk, J.L., Mason, R.P., Obrist, D., Selin, H., Selin, N.E., Thompson, M.R., 2018. A critical time for mercury science to inform global policy. Environ. Sci. Technol. 52, 9556–9561. https://doi.org/10.1021/acs.est.8b02286.

Cheng, L., Zhu, J., Chen, G., Zheng, X., Oh, N.-H., Rufty, T.W., Richter, D.deB., Hu, S., 2010. Atmospheric CO 2 enrichment facilitates cation release from soil. Ecol. Lett.

13, 284–291. https://doi.org/10.1111/j.1461-0248.2009.01421.x.

Clarkson, T.W., Magos, L., 2006. The toxicology of mercury and its chemical compounds. Crit. Rev. Toxicol. 36, 609–662. https://doi.org/10.1080/10408440600845619.

European Food Safety Authority, P. on C. in the F.C. (CONTAM), 2012. Scientific Opinion on the risk for public health related to the presence of mercury and methylmercury in food. EFSA J. 10, 2985. https://doi.org/10.2903/j.efsa.2012.2985.

Farhat, Y.A., Kim, S.-H., Seyfferth, A.L., Zhang, L., Neumann, R.B., 2021. Altered arsenic availability, uptake, and allocation in rice under elevated temperature. Sci. Total Environ. 763, 143049 https://doi.org/10.1016/j.scitotenv.2020.143049.

Guo, J., Zhang, W., Zhang, M., Zhang, L., Bian, X., 2012. Will elevated CO2 enhance mineral bioavailability in wetland ecosystems? Evidence from a rice ecosystem.

Plant Soil 355, 251–263. https://doi.org/10.1007/s11104-011-1096-0.

Hao, Y.Y., Zhu, Y.J., Yan, R.Q., Gu, B., Zhou, X.Q., Wei, R.R., Wang, C., Feng, J., Huang, Q., Liu, Y.R., 2022. Important roles of thiols in methylmercury uptake and translocation by rice plants. Environ. Sci. Technol. 56, 6765–6773. https://doi.org/ 10.1021/acs.est.2c00169.

Haynes, K.M., Kane, E.S., Potvin, L., Lilleskov, E.A., Kolka, R.K., Mitchell, C.P.J., 2019. Impacts of experimental alteration of water table regime and vascular plant community composition on peat mercury profiles and methylmercury production. Sci. Total Environ. 682, 611–622. https://doi.org/10.1016/j.scitotenv.2019.05.072.

Hidayati, N., Triadiati, Anas, I., 2016. Photosynthesis and transpiration rates of rice cultivated under the system of rice intensification and the effects on growth and yield. HAYATI J. Biosci. 23, 67–72. https://doi.org/10.1016/j.hjb.2016.06.002.

Hintelmann, H., Keppel-Jones, K., Evans, R.D., 2000. Constants of mercury methylation and demethylation rates in sediments and comparison of tracer and ambient mercury availability. Environ. Toxicol. Chem. 19, 2204–2211.

Huard, D., Fyke, J., Capellan-P ´ erez, I., Matthews, H.D., Partanen, A.-I., 2022. Estimating ´ the likelihood of GHG concentration scenarios from probabilistic integrated assessment model simulations. Earths Future 10, e2022EF002715. https://doi.org/10.1029/2022EF002715.

Hylander, L.D., Goodsite, M.E., 2006. Environmental costs of mercury pollution. Sci.

Total Environ. 368, 352–370. https://doi.org/10.1016/j.scitotenv.2005.11.029.

Ikawa, H., Chen, C.P., Sikma, M., Yoshimoto, M., Sakai, H., Tokida, T., Usui, Y., Nakamura, H., Ono, K., Maruyama, A., Watanabe, T., Kuwagata, T., Hasegawa, T., 2018. Increasing canopy photosynthesis in rice can be achieved without a large increase in water use—A model based on free-air CO2 enrichment. Glob. Change Biol. 24, 1321–1341. https://doi.org/10.1111/gcb.13981.

IPCC, Masson-Delmotte, V., Zhai, P., Pirani, A., Connors, S.L., P ´ean, C., Berger, S., Caud, N., Chen, Y., Goldfarb, L., Gomis, M.I., Huang, M., Leitzell, K., Lonnoy, E.,

Matthews, J.B.R., Maycock, T.K., Waterfield, T., Yelekçi, O., Yu, R., Zhou, B., 2021.

Summary for Policymakers. Climate Change 2021: The Physical Science Basis. Contribution of Working Group I to the Sixth Assessment Report of the Intergovernmental Panel on Climate Change. IPCC.

Karagas, M.R., Choi, A.L., Oken, E., Horvat, M., Schoeny, R., Kamai, E., Cowell, W., Grandjean, P., Korrick, S., 2012. Evidence on the human health effects of low-level methylmercury exposure. Environ. Health Perspect. 120, 799–806. https://doi.org/10.1289/ehp.1104494.

Keenan, T.F., Hollinger, D.Y., Bohrer, G., Dragoni, D., Munger, J.W., Schmid, H.P., Richardson, A.D., 2013. Increase in forest water-use efficiency as atmospheric carbon dioxide concentrations rise. Nature 499, 324–327. https://doi.org/10.1038/ nature12291.

Khush, G.S., 2005. What it will take to Feed 5.0 Billion Rice consumers in 2030. Plant Mol. Biol. 59, 1–6. https://doi.org/10.1007/s11103-005-2159-5.

Kumar, U., Quick, W.P., Barrios, M., Sta Cruz, P.C., Dingkuhn, M., 2017. Atmospheric CO2 concentration effects on rice water use and biomass production. PloS One 12, e0169706. https://doi.org/10.1371/journal.pone.0169706.

Li, Y., Zhao, J., Zhang, B., Liu, Y., Xu, X., Li, Y.-F., Li, B., Gao, Y., Chai, Z., 2015. The influence of iron plaque on the absorption, translocation and transformation of mercury in rice (Oryza sativa L.) seedlings exposed to different mercury species.

Plant Soil. https://doi.org/10.1007/s11104-015-2627-x.

Li, P., Du, B., Chan, H.M., Feng, X., 2015a. Human inorganic mercury exposure, renal effects and possible pathways in Wanshan mercury mining area, China. Environ. Res. 140, 198–204. https://doi.org/10.1016/j.envres.2015.03.033.

Li, P., Feng, X., Chan, H.-M., Zhang, X., Du, B., 2015b. Human body burden and dietary methylmercury intake: the relationship in a rice-consuming population. Environ. Sci.

Technol. 49, 9682–9689. https://doi.org/10.1021/acs.est.5b00195.

Li, Y., Zhao, J., Guo, J., Liu, M., Xu, Q., Li, H., Li, Y.F., Zheng, L., Zhang, Z., Gao, Y.,

2017. Influence of sulfur on the accumulation of mercury in rice plant (Oryza sativa L.) growing in mercury contaminated soils. Chemosphere 182, 293–300. https://doi. org/10.1016/j.chemosphere.2017.04.129.

Liu, M., Zhang, Q., Cheng, M., He, Y., Chen, L., Zhang, H., Cao, H., Shen, H., Zhang, W., Tao, S., Wang, X., 2019. Rice life cycle-based global mercury biotransport and human methylmercury exposure. Nat. Commun. 10, 5164. https://doi.org/10.1038/ s41467-019-13221-2.

Liu, J., Meng, B., Poulain, Alexandre.J., Meng, Q., Feng, X., 2021. Stable isotope tracers identify sources and transformations of mercury in rice (Oryza sativa L.) growing in a mercury mining area. Fundam. Res. 1, 259–268. https://doi.org/10.1016/j. fmre.2021.04.003.

Maisch, M., Lueder, U., Kappler, A., Schmidt, C., 2019. Iron lung: how rice roots induce iron redox changes in the rhizosphere and create niches for microaerophilic Fe(II)- oxidizing bacteria. Environ. Sci. Technol. Lett. 6, 600–605. https://doi.org/10.1021/acs.estlett.9b00403.

Mao, Q., Tang, L., Ji, W., Rennenberg, H., Hu, B., Ma, M., 2021. Elevated CO2 and soil mercury stress affect photosynthetic characteristics and mercury accumulation of

rice. Ecotoxicol. Environ. Saf. 208, 111605 https://doi.org/10.1016/j. ecoenv.2020.111605.

Meng, B., Feng, X., Qiu, G., Cai, Y., Wang, D., Li, P., Shang, L., Sommar, J., 2010. Distribution patterns of inorganic mercury and methylmercury in tissues of rice (Oryza sativa L.) plants and possible bioaccumulation pathways. J. Agric. Food Chem. 58, 4951–4958. https://doi.org/10.1021/jf904557x.

Meng, B., Feng, X., Qiu, G., Liang, P., Li, P., Chen, C., Shang, L., 2011. The process of methylmercury accumulation in rice (Oryza sativa L.). Environ. Sci. Technol. 45, 2711–2717. https://doi.org/10.1021/es103384v.

Meng, B., Feng, X., Qiu, G., Wang, D., Liang, P., Li, P., Shang, L., 2012. Inorganic mercury accumulation in rice (Oryza sativa L.). Environ. Toxicol. Chem. 31, 2093–2098. https://doi.org/10.1002/etc.1913.

Meng, B., Feng, X., Qiu, G., Anderson, C.W.N., Wang, J., Zhao, L., 2014. Localization and speciation of mercury in brown rice with implications for Pan-Asian public health.

Environ. Sci. Technol. 48, 7974–7981. https://doi.org/10.1021/es502000d.

Meng, M., Li, B., Shao, J., Wang, T., He, B., Shi, J., Ye, Z., Jiang, G., 2014. Accumulation of total mercury and methylmercury in rice plants collected from different mining areas in China. Environ. Pollut. 184, 179–186. https://doi.org/10.1016/j. envpol.2013.08.030.

Millhollen, A.G., Obrist, D., Gustin, M.S., 2006. Mercury accumulation in grass and forb species as a function of atmospheric carbon dioxide concentrations and mercury exposures in air and soil. Chemosphere 65, 889–897. https://doi.org/10.1016/j.chemosphere.2006.03.008.

Muehe, E.M., Wang, T., Kerl, C.F., Planer-Friedrich, B., Fendorf, S., 2019. Rice production threatened by coupled stresses of climate and soil arsenic. Nat. Commun.

10, 4985. https://doi.org/10.1038/s41467-019-12946-4.

Natali, S.M., Sanudo-Wilhelmy, S.A., Norby, R.J., Zhang, H., Finzi, A.C., Lerdau, M.T., ˜ 2008. Increased mercury in forest soils under elevated carbon dioxide. Oecologia 158, 343–354. https://doi.org/10.1007/s00442-008-1135-6.

Neumann, R.B., Seyfferth, A.L., Teshera-Levye, J., Ellingson, J., 2017. Soil warming increases arsenic availability in the rice rhizosphere. Agric. Environ. Lett. 2, 1700062. https://doi.org/10.2134/ael2017.02.0006.

Pierce, C., Psarska, S., Stewart, B.D., Oleheiser, K., Griffiths, N.A., Gutknecht, J.L.M.,

Kolka, R.K., Sebestyen, S.D., Nater, E.A., Toner, B.M., 2022. Whole-Ecosystem Climate Manipulation Effects on Total Mercury within a Boreal Peatland (preprint).

In Review. https://doi.org/10.21203/rs.3.rs-2207553/v1.

R Core Team, 2016. R: A language and environment for statistical computing [WWW Document]. R Found. Stat. Comput, Vienna Austria. URL. https://www.R-project.or g (accessed 9.22.17).

Rho, H., Doty, S.L., Kim, S.-H., 2020. Endophytes alleviate the elevated CO2-dependent decrease in photosynthesis in rice, particularly under nitrogen limitation. J. Exp. Bot.

71, 707–718. https://doi.org/10.1093/jxb/erz440.

Rothenberg, S.E., Feng, X., 2012. Mercury cycling in a flooded rice paddy. J. Geophys.

Res. 117 https://doi.org/10.1029/2011JG001800.

Rothenberg, S.E., Yu, X., Zhang, Y., 2013. Prenatal methylmercury exposure through maternal rice ingestion: Insights from a feasibility pilot in Guizhou Province, China.

Environ. Pollut. 180, 291–298. https://doi.org/10.1016/j.envpol.2013.05.037.

Rothenberg, S.E., Windham-Myers, L., Creswell, J.E., 2014. Rice methylmercury exposure and mitigation: a comprehensive review. Environ. Res. 133, 407–423.

https://doi.org/10.1016/j.envres.2014.03.001.

Rothenberg, S.E., Mgutshini, N.L., Bizimis, M., Johnson-Beebout, S.E., Ramanantsoanirina, A., 2015. Retrospective study of methylmercury and other metal(loid)s in Madagascar unpolished rice (Oryza sativa L.). Environ. Pollut. 196, 125–133. https://doi.org/10.1016/j.envpol.2014.10.002.

Rothenberg, S.E., Yu, X., Liu, J., Biasini, F.J., Hong, C., Jiang, X., Nong, Y., Cheng, Y., Korrick, S.A., 2016. Maternal methylmercury exposure through rice ingestion and offspring neurodevelopment: a prospective cohort study. Int. J. Hyg. Environ. Health 219, 832–842. https://doi.org/10.1016/j.ijheh.2016.07.014.

Rothenberg, S.E., Korrick, S.A., Liu, J., Nong, Y., Nong, H., Hong, C., Trinh, E.P., Jiang, X., Biasini, F.J., Ouyang, F., 2021. Maternal methylmercury exposure through rice ingestion and child neurodevelopment in the first three years: a prospective cohort study in rural China. Environ. Health 20, 50. https://doi.org/10.1186/ s12940-021-00732-z.

Shimono, H., Nakamura, H., Hasegawa, T., Okada, M., 2013. Lower responsiveness of canopy evapotranspiration rate than of leaf stomatal conductance to open-air CO 2 elevation in rice. Glob. Change Biol. 19, 2444–2453. https://doi.org/10.1111/ gcb.12214.

Strickman, R.J., Mitchell, C.P.J., 2017. Accumulation and translocation of methylmercury and inorganic mercury in Oryza sativa: An enriched isotope tracer study. Sci. Total Environ. 574, 1415–1423. https://doi.org/10.1016/j.

scitotenv.2016.08.068.

Strickman, R.J., Larson, S., Huang, H., Kakouros, E., Marvin-DiPasquale, M., Mitchell, C. P.J., Neumann, R.B., 2022. The relative importance of mercury methylation and demethylation in rice paddy soil varies depending on the presence of rice plants.

Ecotoxicol. Environ. Saf. 230, 113143 https://doi.org/10.1016/j. ecoenv.2021.113143.

Syversen, T., Kaur, P., 2012. The toxicology of mercury and its compounds. J. Trace Elem. Med. Biol. 26, 215–226. https://doi.org/10.1016/j.jtemb.2012.02.004.

Tang, B., Chen, J., Wang, Z., Qin, P., Zhang, X., 2021. Mercury accumulation response of rice plant (Oryza sativa L.) to elevated atmospheric mercury and carbon dioxide.

Ecotoxicol. Environ. Saf. 224, 112628 https://doi.org/10.1016/j. ecoenv.2021.112628.

Tanner, K.C., Windham-Myers, L., Marvin-DiPasquale, M., Fleck, J.A., Tate, K.W.,

Linquist, B.A., 2018. Methylmercury dynamics in upper sacramento valley rice fields with low background soil mercury levels. J. Environ. Qual. 47, 830. https://doi.org/ 10.2134/jeq2017.10.0390.

Taylor, G.J., Crowder, A.A., 1983. Use of the DCB technique for extraction of hydrous iron oxides from roots of wetland plants. Am. J. Bot. 70, 1254–1257.

Tiffreau, C., Lutzkirchen, J., Behra, P., 1995. Modeling the adsorption of mercury (II) on (Hydr) oxides. J. Colloid Interface Sci. 172, 82–93.

Ullrich, S.M., Tanton, T.W., Abdrashitova, S.A., 2001. Mercury in the aquatic environment: A review of factors affecting methylation. Crit. Rev. Environ. Sci.

Technol. 31, 241–293. https://doi.org/10.1080/20016491089226.

United States Environmental Protection Agency, 2001. Method 1630. Methyl Mercury in Water by Distillation, Aqueous Ethylation, Purge and Trap, and CVAFS, EPA 821-R- 01- 020.

Washington, DC. https://www.epa.gov/sites/default/files/2015-08/documents /method_1630_1998.pdf.

United States Environmental Protection Agency, 2002. Method 1631. Revision E: Mercury in Water by Oxidation, Purge andTrap, and Cold Vapor Atomic Fluorescence Spectrometry. Washington, DC. https://www.epa.gov/sites/default/files/2015-08/ documents/method_1631e_2002.pdf.

United States Environmental Protection Agency, 2007. Method 7473. Mercury in Solids and Solutions by Thermal Decomposition Amalgamation, and Atomic Absorption Spectrophotometry. Washington, DC. https://www.epa.gov/esam/epa-method-7473-s w-846-mercury-solids-and-solutions-thermal-decomposition-amalgamation-and.

Verma, P.K., Verma, S., Pandey, N., 2022. Root system architecture in rice: impacts of genes, phytohormones and root microbiota. 3 Biotech 12, 239. https://doi.org/ 10.1007/s13205-022-03299-9.

Viˇsnjevec, A.M., Kocman, D., Horvat, M., 2014. Human mercury exposure and effects in Europe. Environ. Toxicol. Chem. 33, 1259–1270. https://doi.org/10.1002/etc.2482.

Wang, Y., Frei, M., Song, Q., Yang, L., 2011. The impact of atmospheric CO2 concentration enrichment on rice quality – A research review. Acta Ecol. Sin. 31, 277–282. https://doi.org/10.1016/j.chnaes.2011.09.006.

Wang, X., Li, B., Tam, N.F.Y., Huang, L., Qi, X., Wang, H., Ye, Z., Meng, M., Shi, J., 2014. Radial oxygen loss has different effects on the accumulation of total mercury and methylmercury in rice. Plant Soil. https://doi.org/10.1007/s11104-014-2239-x.

Wang, X., Tam, N.F.Y., He, H., Ye, Z., 2015. The role of root anatomy, organic acids and iron plaque on mercury accumulation in rice. Plant Soil 394, 301–313. https://doi. org/10.1007/s11104-015-2537-y.

Wang, Y., Habibullah-Al-Mamun, M., Han, J., Wang, L., Zhu, Y., Xu, X., Li, N., Qiu, G., 2020. Total mercury and methylmercury in rice: Exposure and health implications in Bangladesh. Environ. Pollut. 265, 114991 https://doi.org/10.1016/j.

envpol.2020.114991.

Wang, B., Chen, M., Ding, L., Zhao, Y., Man, Y., Feng, L., Li, P., Zhang, L., Feng, X., 2021. Fish, rice, and human hair mercury concentrations and health risks in typical Hg-contaminated areas and fish-rich areas, China. Environ. Int. 154, 106561 https:// doi.org/10.1016/j.envint.2021.106561.

Wang, Y., Wang, X., Ai, F., Du, W., Yin, Y., Guo, H., 2023. Climatic CO2 level-driven changes in the bioavailability, accumulation, and health risks of Cd and Pb in paddy soil–rice systems. Environ. Pollut. 324, 121396 https://doi.org/10.1016/j. envpol.2023.121396.

Windham-Myers, L., Marvin-Dipasquale, M., Krabbenhoft, D.P., Agee, J.L., Cox, M.H., Heredia-Middleton, P., Coates, C., Kakouros, E., 2009. Experimental removal of wetland emergent vegetation leads to decreased methylmercury production in surface sediment. J. Geophys. Res. 114 https://doi.org/10.1029/2008JG000815.

Wu, H., Tang, S., Zhang, X., Guo, J., Song, Z., Tian, S., Smith, D.L., 2009. Using elevated CO2 to increase the biomass of a Sorghum vulgare×Sorghum vulgare var. sudanense hybrid and trifolium pratense L. and to trigger hyperaccumulation of cesium. J. Hazard. Mater. 170, 861–870. https://doi.org/10.1016/j.jhazmat.2009.05.069.

Wu, C., Wu, G., Wang, Z., Zhang, Z., Qian, Y., Ju, L., 2018. Soil mercury speciation and accumulation in rice (Oryza sativa L.) grown in wastewater-irrigated farms. Appl.

Geochem. 89, 202–209. https://doi.org/10.1016/j.apgeochem.2017.12.009. Xu, X., Zhao, J., Li, Y., Fan, Y., Zhu, N., Gao, Y., Li, B., Liu, H., Li, Y.F., 2016. Demethylation of methylmercury in growing rice plants: An evidence of self- detoxification. Environ. Pollut. 210, 113–120. https://doi.org/10.1016/j. envpol.2015.12.013.

Xu, X., Yan, M., Liang, L., Lu, Q., Han, J., Liu, L., Feng, X., Guo, J., Wang, Y., Qiu, G., 2019. Impacts of selenium supplementation on soil mercury speciation, and inorganic mercury and methylmercury uptake in rice (Oryza sativa L.). Environ.

Pollut. 249, 647–654. https://doi.org/10.1016/j.envpol.2019.03.095.

Yang, Z., Fang, W., Lu, X., Sheng, G.-P., Graham, D.E., Liang, L., Wullschleger, S.D., Gu, B., 2016. Warming increases methylmercury production in an arctic soil.

Environ. Pollut. 214, 504–509. https://doi.org/10.1016/j.envpol.2016.04.069.

Yang, X., Wang, D., Tao, Y., Shen, M., Wei, W., Cai, C., Ding, C., Li, J., Song, L., Yin, B., Zhu, C., 2022. Effects of elevated CO2 on the Cd uptake by rice in Cd-contaminated paddy soils. J. Hazard. Mater. 130140 https://doi.org/10.1016/j.

jhazmat.2022.130140.

Yang, X., Wang, D., Tao, Y., Shen, M., Ma, C., Cai, C., Song, L., Yin, B., Zhu, C., 2023. Does elevated CO2 enhance the arsenic uptake by rice? Yes or maybe: evidences from FACE experiments. Chemosphere 327, 138543. https://doi.org/10.1016/j. chemosphere.2023.138543.

Zandi, P., Yang, J., Darma, A., Bloem, E., Xia, X., Wang, Y., Li, Q., Schnug, E., 2023. Iron plaque formation, characteristics, and its role as a barrier and/or facilitator to heavy metal uptake in hydrophyte rice (Oryza sativa L.). Environ. Geochem. Health 45, 525–559. https://doi.org/10.1007/s10653-022-01246-4.

Zhang, L., Qiu, Y., Cheng, L., Wang, Y., Liu, L., Tu, C., Bowman, D.C., Burkey, K.O., Bian, X., Zhang, W., Hu, S., 2018. Atmospheric CO2 Enrichment and Reactive Nitrogen Inputs Interactively Stimulate Soil Cation Losses and Acidification.

Environ. Sci. Technol. 52, 6895–6902. https://doi.org/10.1021/acs.est.8b00495.

Zhang, C., Gan, C., Ding, L., Xiong, M., Zhang, A., Li, P., 2020. Maternal inorganic mercury exposure and renal effects in the Wanshan mercury mining area, southwest China. Ecotoxicol. Environ. Saf. 189, 109987 https://doi.org/10.1016/j. ecoenv.2019.109987.

Zhao, J.Y., Ye, Z.H., Zhong, H., 2018. Rice root exudates affect microbial methylmercury production in paddy soils. Environ. Pollut. 242, 1921–1929. https://doi.org/ 10.1016/j.envpol.2018.07.072.

Zhou, X.B., Li, Y.Y., 2019. Effect of iron plaque and selenium on mercury uptake and translocation in rice seedlings grown in solution culture. Environ. Sci. Pollut. Res. 26, 13795–13803. https://doi.org/10.1007/s11356-018-3066-z.

Zhou, J., Obrist, D., 2021. Global Mercury Assimilation by Vegetation. Environ. Sci.

Technol. 55, 14245–14257. https://doi.org/10.1021/acs.est.1c03530.

Zhou, J., Liu, H., Du, B., Shang, L., Yang, J., Wang, Y., 2015. Influence of soil mercury concentration and fraction on bioaccumulation process of inorganic mercury and methylmercury in rice (Oryza sativa L.). Environ. Sci. Pollut. Res. 22, 6144–6154. https://doi.org/10.1007/s11356-014-3823-6.